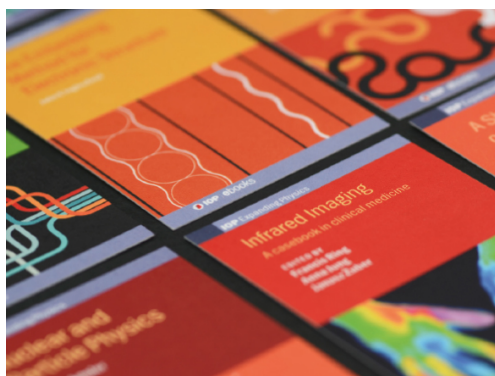# Critical minima in elastic electron scattering by argon

To cite this article: R Panajotovic *et al* 1997 *J. Phys. B: At. Mol. Opt. Phys.* **30** 5877

View the article online for updates and enhancements.

Critical minima in elastic electron scattering by argon

R Panajotović†, D Filipović†§, B Marinković†, V Pejčev†, M Kurepa†§ and L Vušković‡

† Institute of Physics, PO Box 57, 11001 Belgrade, Yugoslavia
‡ Physics Department, Old Dominion University, Norfolk, VA 23529, USA

Abstract. We determined experimentally two critical points in elastic electron scattering by argon where the differential cross section (DCS) attains its smallest values. The points were found to be at $68.5° \pm 0.3°$, 41.30 ± 0.02 eV and at $143.5° \pm 0.3°$, 37.30 ± 0.02 eV. Special attention was given to improve the angular resolution in order to determine the exact positions of the minima. These minima are important because they are a sensitive test of the validity of experimental procedures, and are used to verify theoretical predictions of DCS shapes and magnitudes, and of the polarization of scattered electrons. Normalized DCS were determined by measuring the angular distributions of elastically scattered electrons at incident energies of 10, 15, 20, 25, 30, 40, 50, 60, 75, 80, 90 and 100 eV in the angular range $20°$–$150°$. Results are compared with the available experimental and theoretical data. In addition, integral, momentum-transfer, and viscosity cross sections were determined by numerical integration of the measured DCS extrapolated to $0°$ and to $180°$.

1. Introduction

There is a long standing need to determine critical points in elastic electron scattering by argon where the differential cross section (DCS) attains its smallest values. These minima are important because they are a sensitive test of the validity of experimental procedures, as well as of theoretical predictions of DCS shapes, magnitudes, and dependence on the polarization of the scattered electrons. The DCS for electron scattering by argon has been extensively examined since the first electron scattering experiments were performed in a wider angular range (Bullard and Massey 1931, Hughes and McMillen 1932). Relative or absolute values of the elastic DCS have been measured at low (Dehmel *et al* 1976, Haddad and O'Malley 1982, Weyhreter *et al* 1988, Furst *et al* 1989, Gibson *et al* 1996), intermediate (Mehr 1967, Schackert 1968, Lewis *et al* 1974, Williams and Willis 1975, Vušković and Kurepa 1976, DuBois and Rudd 1976, Srivastava *et al* 1981, Qing *et al* 1982, Cvejanović and Crowe 1994, 1997, Crowe and Cvejanović 1996), and high (Mehr 1967, DuBois and Rudd 1976, Bromberg 1974, Gupta and Rees 1975, Jansen *et al* 1976) impact energies. A representative table of theoretical critical points calculated by different approximations was given by Lucas (1979, table 2). At the same time, the energy and angular separations in the measurements are too large to find the exact positions of prominent minima.

Plotting the positions of DCS minima as a function of the incident electron energy is a convenient way to compare experimental data with calculated results. The reason is that differences in the minima positions versus the energy are more sensitive to experimental

§ Permanent address: Faculty of Physics, University of Belgrade, PO Box 368, 11001 Belgrade, Yugoslavia.

and computational uncertainties than differences in DCS values versus the scattering angle. This is clearer if, for both cases, data are presented in linear–linear instead of in semilog diagrams, used most often for DCS presentation. The explanation for this sensitivity lies in the fact that positions of DCS minima are influenced by contributions from the different electron–atom interaction potentials used in the calculation. Calculated positions of DCS minima are very sensitive to the choice of the atomic potential with which the calculation has been performed. On the other hand, the polarization of the scattered electrons possesses a maximum in the vicinity of DCS minima, and it also changes drastically within a small angular interval around the DCS minimum. Calculated results of electron polarization, including total polarization, were shown to be very sensitive to both the scattering angle and the electron energy (Bühring 1968a, Kemper *et al* 1985). For that reason, in order to extract the relevant parameters one needs accurate measurements of both DCS and polarization (Bühring 1968a).

The physical interpretation of DCS minima is much easier when a polarization analysis of scattered electrons is included. Large polarization occurs around a deep DCS minimum. In addition, the sign of the polarization changes within a small angular region around the minimum. In general, the position of the DCS minimum is relatively weakly influenced by the exchange interaction. However, it should be considered whether the exchange substantially affects the nature of the scattering. For example, only the spin-flip process contributes to the spin exchange of scattered electrons in the case of elastic electron scattering by rare-gas atoms in their ground states. Thus, for the rare gases the spin-flip process can be predominant in determining the positions of DCS minima. According to Bühring (1968b), the energy values corresponding to the deepest minima may serve as the significant figures which contain information on and are sensitive to the parameters of the atomic field. These values are called critical energies. Walker (1971) has calculated polarization contours for electron–argon scattering showing the existence of four energy regions where polarization changes drastically. These energy regions closely resemble the positions of critical energies. Lucas (1979) and Khare and Raj (1980) have proposed methods to search for the critical points, which are defined as pairs of incident energy and scattering angle where DCS minima attain their smallest values.

Our aim in this work was to determine the angular positions of DCS minima with improved angular resolution and to experimentally determine the energies of the deepest DCS minima. In addition, we obtained normalized absolute DCSs, as well as the corresponding integral (Q_i), momentum transfer (Q_m) and viscosity (Q_v) cross sections for a number of chosen incident electron energies in the intermediate energy region. Argon was chosen as a target for two reasons. First, it has deep DCS minima in this energy region, which is convenient for the control and improvement of angular resolution. Second, results at some incident electron energies can be compared with DCS results available in the literature.

Published experiments in the electron energy range 10–100 eV, which are relevant to our investigation, can be divided into two groups. In the first group a procedure for obtaining good angular resolution in the DCS measurements was presented (Lewis *et al* 1974, Williams and Willis 1975, DuBois and Rudd 1976, Srivastava *et al* 1981). In the second group the main subject was the polarization analysis of scattered electrons (Mehr 1967, Schackert 1968, Qing *et al* 1982) or the energy dependence of the cross section at a given scattering angle (Cvejanović and Crowe 1994). In the second group, in contrast to the first, a compromise had to be achieved between good resolution and the statistical error due to low signal intensity. As a consequence, results in this second group of measurements have poorer angular resolution. A survey of the available results, classified with respect to

Table 1. Survey of experimental elastic DCS results for electron scattering by argon. Group 1, higher angular resolution; group 2, lower angular resolution.

Experiment	Energy region (eV)	Angular range (degrees)	Angular resolution (degrees)
Group 1			
Lewis *et al* (1974)	15–200	20–140	3
Williams and Willis (1975)	20–400	20–150	±2
DuBois and Rudd (1976)	20–800	5–150	≃2
Srivastava *et al* (1981)	3–100	20–135	±2
This work	10–100	20–150	±1.5
Group 2			
Mehr (1967)	5–1000	30–155	⩾3
Schackert (1968)	40–150	45–155	±3
Qing *et al* (1982)	10–50	40–110	⩾ ±4.5
Cvejanović and Crowe (1994)	20–110	40–120	±3[a]

[a] We estimated the resolution since the apparatus was tuned for measuring the energy dependence of the cross section.

angular resolution in these two groups of papers, is given in table 1.

To cover the energy ranges of experiments in table 1, the relevant DCS calculations (Kemper *et al* 1985, Walker 1971, McEachran and Stauffer 1983, Bartschat *et al* 1994, Mimnagh *et al* 1993, Nahar and Wadehra 1987, Fon *et al* 1983, Saha 1991, Sienkiewicz and Baylis 1987, Haberland *et al* 1986, Plenkiewicz *et al* 1988, Ihra and Friedrich 1992) include various scattering potentials. Kemper *et al* (1985) (10–50 eV) applied a nonlocal, two-channel calculation including polarization to obtain the DCS. Walker (1971) (2–400 eV) performed relativistic calculations, including exchange and distortion. McEachran and Stauffer (1983) (3–50 eV) used the adiabatic-exchange (AE) approximation, including polarization and a local exchange interaction, while Bartschat *et al* 1988 (20–100 eV) used the orbital polarization method with static polarization and exchange included. Mimnagh *et al* (1993) extended the AE calculation to include dynamic-distortion (DD) effects in elastic scattering by argon. Though they obtained the position of the Ramsauer–Townsend minimum in better agreement with experimental data than did their previous AE result, there are still some discrepancies at larger energies. Nahar and Wadehra (1987) (3–300 eV) applied phase shift analysis and Born approximation with a model potential representation. Fon *et al* (1983) (3–150 eV) used *R*-matrix calculations with polarization included. Saha (1991) (3–50 eV) used the multiconfiguration Hartree–Fock method with polarization. Sienkiewicz and Baylis (1987) (0.1–40 eV) used the relativistic Hartree–Fock with polarization and exchange. Haberland *et al* (1986) (5–100 eV) used the Kohn–Sham one-particle approximation with exchange-correlation. Finally, Plenkiewicz *et al* (1988) (0–20 eV) used a pseudopotential approach and Ihra and Friedrich (1992) (0–20 eV) applied a simple local one-parameter potential to determine partial phase shifts and the DCS for elastic scattering of electrons by argon.

The experimental procedure used in this work is described in section 2. Results of the DCS integrated cross sections, and positions of DCS minima as a function of electron energy are presented in section 3 in the form of tables and figures. In the same section is given a discussion of error limits for the determination of these quantities. In section 4 the results are discussed and conclusions given.

2. Experiment

2.1. Experimental set-up

The electron spectrometer used in these experiments is described in detail in Filipović *et al* (1988a). In brief, the angular distributions of elastically scattered electrons were measured by a cross-beam technique. The atomic beam was crossed perpendicularly by a mono-energetic electron beam and the elastically scattered electron intensity was measured as a function of the scattering angle (θ), at a fixed impact energy (E_0). The electron beam was prepared by an electron monochromator which consists of systems of cylindrical electrostatic lenses and a hemispherical electrostatic energy selector. A hairpin thermo-electron source was used. Electrons scattered by the argon atoms were energy analysed by a hemispherical energy analyser rotatable around the atomic beam axis from $-30°$ to $150°$ with respect to the incoming electron beam, and only the elastically scattered electrons were detected by a single-channel electron multiplier. The overall electron energy resolution was about 50 meV, and nominal E_0 was calibrated with respect to the resonance in the elastic channel. Differential pumping of both the electron monochromator and the electron energy analyser with respect to the main vacuum chamber in which the interaction volume is located, ensures substantially lower pressure within the electron-optical system. The background pressure was 2×10^{-3} Pa, under normal operating conditions. The atomic-beam number density within the effective interaction volume was in the range where a linear dependence could be verified between the scattered electron signal intensity and the gas needle reservoir back pressure. Under this condition, the contribution of double electron scattering can be neglected. The background signal contribution to measured scattered electron intensities was tested by closing the inlet valve. As a result, the background pressure decreased to 2×10^{-5} Pa, while the count rate at $\theta = 20°$ diminished to below 1% of the signal under normal operating conditions. This test proved that the background contributions to the measured signal intensities at $\theta \geqslant 20°$ could be neglected.

2.2. Energy calibration

The best way to calibrate the energy scale is to perform the measurements on sharp resonance structures, if those exist, on the same atom which is investigated and in an energy range as close to the investigated range as possible. The use of measurements on the well known resonance structure on helium (the $^2S_{1/2}$ state in He at 19.31 eV) (see e.g. Buckman and Clark 1994) suffers from possible uncertainties due to contact potentials in two different gases (helium and argon). On the other hand, the positions of the two well understood resonances in argon at 11.08 and 11.27 eV are relatively far from the energy region where we were searching for the critical points in the elastic DCS.

  Most investigations of structures in elastic electron–argon scattering have been done by considering low-lying structures in the resonance spectra (Read *et al* 1976, Brunt *et al* 1977). These states could be more easily distinguished and classified than those above the first ionization potential (15.755 eV) where the presence of structures that originate from the excitation of neutral autoionizing states highly complicates the work. Identification of states in such kinds of spectra is possible only if the appropriate coupling scheme is applied. In our experiment we searched for resonances in the elastic channel at $\theta = 10°$, in the energy region 27.8–30.0 eV (see figure 1). Our main objective was to determine the position and width of the most prominent structure at 29.0 eV in order to calibrate the incident electron energy scale.
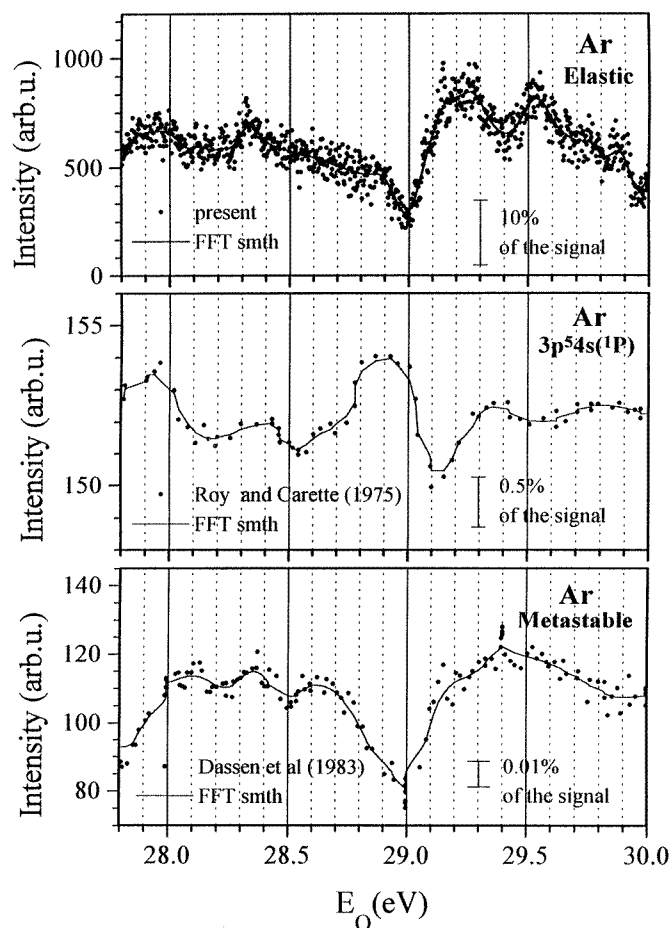
Figure 1. Scattering intensities as a function of incident electron energies: (*a*) our result for the elastic electron–argon scattering at $\theta = 10°$; (*b*) the result of Roy and Carette (1975) for the excitation of the singlet P state (11.83 eV) in the forward direction; (*c*) the result of Dassen *et al* (1983) for the metastable yield. In order to show existing structures fast Fourier transform (FFT) smoothing was applied to all three results and shown as a full curve.

Sanche and Schulz (1972) performed an experiment where the broad energy region 24–32 eV allowed them to observe features with energy losses above the value of the first ionization limit. They observed three structures which they identified as resonances: at 26.84–26.90 eV, 27.87–27.95 eV and 28.82–28.98 eV. This conclusion was supported by the fact that there were no autoionizing states having the same energy as these structures. The other investigation of these structures was made by Roy and Carette (1975). They observed resonances in the excitation function of the $3p^5 4s(^1P)$ state of argon in the energy region 24–32 eV in the forward direction. The authors did not give any designation for the resonances above 27 eV, although they observed several features in that energy region among which the structure at 28.88–29.10 eV was the strongest. Many different structures could be found in the work of Dassen *et al* (1983) who measured the metastable yield of argon atoms in a similar energy region (24–33 eV). Among the other structures they identified in the obtained spectrum, they suggested a classification for the resonances observed by Sanche

and Schulz (1972): for the one at 27.08 eV $[3s^23p^4](^3P)4s^24p$, for the one at 27.88 eV $[3s3p^6](^2S)5s5p(^2P)$, and for the most prominent one at 28.98 eV $[3s^23p^4](^1D)4s^24p$. Only the second resonance had a symmetry suggestion (P-symmetry). Also, data were not taken at different angles to show the behaviour of these resonances in the elastic channel. Buckman and Clark (1994) concluded that resonances in the autoionizing region could be equally associated with the parent states with cores $nsnp^6(^2S)$ and $ns^2np^4(^1S, \,^1D, \,^3P)$. For argon, the ^3P–^1D and ^1D–^1S splitting is 1.7 and 2.4 eV, respectively.

For determination of the position and width of the resonance close to 29 eV we used a fitting method applied earlier on cadmium resonances (Panajotović *et al* 1994). We determined the energy of the resonance to be 29.03 eV and obtained its width of 130 meV. Comparison with the results by Roy and Carette (1975) and by Dassen *et al* (1983) shows that one structure at 28.3 eV coincides with the structure classified as $[3s^23p^4](^3P)4s4p^2$ (Dassen *et al* 1983). There is approximately 100 meV difference between the position of this structure and the similar one, observed in the excitation function (Dassen *et al* 1983). At present, we cannot give a better identification of the other visible features in our elastic spectra since the one at 27.9 eV is rather broad.

2.3. Angular calibration

In this experiment, special attention was given to accurate determination of the scattering angles. The true zero scattering angle was determined from the symmetry of the scattering signals in the $-30°$ to $+30°$ angular region. Typical deviation with respect to the instrumental zero was found to be within $\pm 0.5°$. The correction was made for each angular distribution measurement.

The angle at which the intensity of the primary electron beam falls to half maximum was $\pm 1°$. The angular resolution was carefully considered and experimentally checked to be within $\pm 1.5°$. The atomic beam was well collimated by a 2.5 cm long, 0.05 cm diameter needle (Pt–Ir single tube) with a back pressure of about 13.3 Pa. The centre of the interaction region was 2 mm above the needle. Also, the angular resolution was indirectly tested in measurements of elastic electron scattering by xenon (Marinković *et al* 1983) applying the same apparatus as in this experiment. Excellent agreement in shape between our DCS results and the measurements of Register *et al* (1986) performed with a xenon beam generated by a capillary array, confirmed our angular resolution measurements. It is important to make an additional remark about the angular resolution in the case of deep minima obtained in this work. The DCS final results in the minima are slightly higher than in the best single measurement, due to an averaging procedure which was used in order to obtain more accurate positions of these DCS minima.

2.4. Averaging and normalization procedures

At least five elastically scattered electron angular distributions were measured at each incident energy. From the set of these distributions, at a given incident electron energy, the weighted arithmetic mean value was obtained. The curves so obtained are corrected for effective path length in order to determine the relative DCS. The effective path length correction factors (Brinkmann and Trajmar 1981) were calculated taking into account the following conditions: (a) the large-aspect-ratio tube ($\gamma = 0.02$), (b) the DCS, which decreases by three orders of magnitude from $0°$ to $90°$ scattering angle, and (c) extrapolation to a tube back pressure of 13.3 Pa. The set of correction factors used in this work is given in table 1 of Filipović *et al* (1988b).

The essence of our work was the measurement of relative DCSs in order to obtain minima in elastic scattering. It was divided into two groups of measurements. The first one consists of DCS measurements from 10 to 100 eV, in 5, 10 and 15 eV increments. We present these absolute DCSs normalized with respect to the results of Srivastava *et al* (1981) at the local DCS maximum for a given incident electron energy. These data were chosen for normalization due to the several overlapping incident energies, while the rest of the DCS were normalized with respect to the interpolated local DCS maximum plotted as a function of incident energy. The second group of measurements are those which closely examine the energy region 30–60 eV in order to search for minima positions and critical points.

Integrated cross sections were obtained by numerical integration of our DCSs in the angular range 20°–150°, extrapolated to 0° and 180°. The extrapolation procedure was the same as in Filipović *et al* (1988b).

3. Results and discussion

3.1. Elastic DCSs

We have measured angular distributions of electrons elastically scattered by argon between 20° and 150° at incident electron energies of 10, 15, 20, 25, 30, 40, 50, 60, 75, 80, 90, and 100 eV. Our results are presented in table 2. In figure 2(*a*) a three-dimensional representation of the DCS(E_0, θ) surface is shown on a logarithmic scale, while the projection on the horizontal plane is shown in figure 2(*b*). Results at 20 eV and 60 eV are chosen to compare with available theoretical and experimental data, which are presented in figures 3 and 4, respectively. A satisfactory agreement in shape can be seen, except for the positions of the DCS minima. However, there are some differences in absolute values.

The total error in these normalized DCSs is estimated to be 22%. Contributions to this error are due to statistical error (5%), effective path-length correction (5%), normalization of relative to absolute DCSs (5%) and the error in absolute values used for normalization (20% as quoted by Srivastava *et al* (1981)). The statistical errors at some angles around local minima were larger than 5% due to very low signal intensity, resulting in a slightly higher total error than quoted.

3.2. Integrated cross sections

Integrated cross sections, Q_i, Q_m, and Q_v, defined as

$$Q_i(E_0) = 2\pi \int_0^\pi \sigma(\theta) \sin\theta \, d\theta \tag{1}$$

$$Q_m(E_0) = 2\pi \int_0^\pi \sigma(\theta)(1 - \cos\theta) \sin\theta \, d\theta \tag{2}$$

$$Q_v(E_0) = 2\pi \int_0^\pi \sigma(\theta)(1 - \cos^2\theta) \sin\theta \, d\theta \tag{3}$$

are calculated by numerical integration of DCSs, extrapolated to 0° and 180°. Our results are presented in table 3. Errors in the integrated cross sections are estimated to be 30%. In addition to the error in the measured DCS, there are errors caused by the extrapolation procedure to angles lower than 20° and larger than 150° (10%), and numerical integration (5%). A comparison of results from table 3 with other available data will be presented in a future publication where we will elaborate on the possibility of using total and integral cross sections to obtain more accurate normalized absolute elastic DCSs for electron scattering by argon.

Table 2. Elastic differential cross sections for electron scattering by argon in units of 10^{-20} m^2 sr^{-1} as a function of scattering angle (listed down left-hand column) and E_0 (indicated in eV across the top of the table). The numbers in parentheses are extrapolations.

θ (deg)	10.3	15.3	20.3	25.3	30.3	40.3	50.3	60.3	75.3	80.3	90.3	100.3
20	8.09	10.10	8.43	8.26	8.01	7.45	4.81	4.51	2.70	3.20	2.53	1.94
25	6.36	9.46	7.48	6.71	6.02	5.72	3.18	3.07	1.72	1.72	1.46	1.12
30	4.89	7.17	6.12	5.42	4.11	3.73	2.27	1.98	1.05	1.05	0.77	0.61
35	3.92	5.53	4.64	4.19	3.30	2.63	1.43	1.13	0.60	0.68	0.43	0.36
40	2.91	4.27	3.45	2.91	2.27	1.81	0.90	0.75	0.30	0.33	0.23	0.22
45	2.41	2.97	2.32	2.04	1.58	1.15	0.54	0.36	0.18	0.18	0.13	0.12
50	1.69	1.79	1.51	1.22	1.04	0.61	0.30	0.17	0.085	0.094	0.079	0.075
55	1.33	1.05	0.90	0.73	0.52	0.34	0.13	0.075	0.041	0.045	0.052	0.061
57											0.051	
58												0.058
60	1.06	0.58	0.48	0.33	0.19	0.14	0.040	0.029	0.027	0.034	0.053	0.060
64								0.0135				
65	0.93	0.40	0.20	0.12	0.075	0.030	0.009	0.014	0.038	0.040	0.067	0.070
68						0.012						
70	0.88	0.30	0.073	0.034	0.016	0.015	0.026	0.037	0.057	0.059	0.092	0.082
71		0.30										
72			0.051	0.028								
75	0.89	0.33	0.063	0.043	0.069	0.059	0.084	0.082	0.087	0.089	0.12	0.099
80	0.87	0.43	0.15	0.11	0.14	0.14	0.15	0.13	0.12	0.12	0.14	0.12
85	0.86	0.55	0.26	0.21	0.25	0.23	0.23	0.28	0.16	0.15	0.15	0.13
90	0.78	0.60	0.37	0.32	0.34	0.30	0.29	0.24	0.18	0.17	0.16	0.12
94		0.62										
95	0.62	0.61	0.44	0.42	0.41	0.36	0.33	0.26	0.19	0.18	0.16	0.11
100	0.44	0.57	0.48	0.48	0.47	0.40	0.33	0.27	0.20	0.17	0.13	0.094
104						0.40						
105	0.27	0.49	0.46	0.50	0.44	0.40	0.32	0.25	0.15	0.15	0.089	0.069
110	0.12	0.39	0.43	0.46	0.42	0.37	0.28	0.20	0.11	0.12	0.060	0.044
115	0.058	0.35	0.37	0.40	0.36	0.32	0.22	0.15	0.078	0.068	0.033	0.027
118		0.32										
120	0.11	0.33	0.31	0.34	0.27	0.25	0.16	0.10	0.042	0.045	0.014	0.009
121											0.012	
123												0.007
125	0.30	0.45	0.24	0.24	0.20	0.17	0.11	0.065	0.026	0.025	0.016	0.010
128									0.022			
129										0.020		
130	0.56	0.62	0.21	0.17	0.13	0.10	0.068	0.050	0.025	0.022	0.044	0.040
134								0.038				
135	1.02	0.91	0.22	0.12	0.063	0.059	0.045	0.046	0.046	0.046	0.10	0.082
138							0.036					
140	1.54	1.27	0.28	0.11	0.036	0.026	0.044	0.078	0.090	0.091	0.16	0.15
141				0.10								
142					0.033							
143						0.017						
145	2.32	1.69	0.37	0.11	0.040	0.018	0.076	0.13	0.16	0.18	0.22	0.25
148	2.62	1.87	0.42						0.19			
150	(2.7)	(2.0)	(0.45)	0.16	0.059	0.041	0.14	0.23	(0.2)	0.24	(0.25)	0.32

3.3. Positions of DCS minima

Two areas of deep DCS minima existing in the considered energy domain can be seen in figure 2(*b*). In these areas are located the critical points in elastic electron–argon scattering

Table 3. Integral (Q_i), momentum transfer (Q_m), and viscosity (Q_v) cross sections for elastic electron scattering by argon in units of 10^{-20} m^2.

E_0 (eV)	10.3	15.3	20.3	25.3	30.3	40.3	50.3	60.3	75.3	80.3	90.3	100.3
Q_i	19.8	21.0	16.0	13.7	12.0	9.5	7.1	6.4	4.0	4.3	3.8	3.5
Q_m	12.5	11.3	5.6	4.4	3.7	3.0	2.4	2.6	1.6	1.5	1.5	1.4
Q_v	7.9	7.6	5.4	4.6	4.0	3.2	2.3	1.7	1.2	1.2	1.1	0.9

Table 4. Elastic differential cross sections for electron scattering by argon in units of 10^{-23} m^2 sr^{-1}. The numbers in parentheses are absolute errors.

θ (deg)	40.3 eV	41.3 eV	42.3 eV	43.3 eV	44.3 eV
64	42.1(4.6)	41.0(6.1)	25.8(5.5)	38.3(5.6)	41.3(7.9)
65	29.6(3.5)	26.8(4.8)	17.7(4.4)	26.0(5.1)	29.9(5.8)
66	20.7(2.4)	16.5(3.4)	11.9(3.5)	17.2(4.0)	21.2(4.1)
67	15.1(1.5)	9.8(2.5)	8.4(2.3)	11.5(3.1)	15.0(2.9)
67.5	13.4(1.1)	7.7(1.9)	7.4(2.0)	9.8(2.4)	12.8(2.6)
68	12.5(0.9)	6.5(1.5)	6.9(1.9)	8.7(2.0)	11.3(2.4)
68.5	12.2(0.8)	6.1(1.3)	6.9(1.9)	8.4(1.9)	10.5(2.1)
69	12.5(1.0)	6.6(1.5)	7.4(2.1)	8.6(2.0)	10.3(2.1)
69.5	13.5(1.2)	7.8(1.8)	8.3(2.2)	9.5(2.2)	10.7(2.1)
70	15.1(1.5)	9.8(2.2)	9.7(2.3)	11.0(2.5)	11.8(2.1)
71	20.0(2.2)	16.1(3.4)	13.7(2.9)	15.6(3.5)	15.8(2.6)
72	27.0(3.0)	25.2(4.6)	19.4(3.4)	22.2(4.3)	22.4(3.4)
73	35.9(3.4)	37.2(5.8)	26.5(4.3)	30.7(4.8)	31.6(4.3)
74	46.6(3.9)	51.9(6.8)	35.1(5.2)	40.9(5.7)	43.4(5.7)

where the cross section attains its smallest value at some particular incident energy and scattering angle. In order to determine the exact positions of critical points it was necessary to examine thoroughly the 30–60 eV region of incident energies and 60°–150° region of scattering angles. We measured the DCS in 1 eV increments in the ranges 36.3–44.3 eV and 53.3–58.3 eV. Results are shown for the low-angle minimum in figure 5 and table 4, and for the high-angle minimum in figure 6 and table 5. For each energy several sets of measurements were taken at angles around the minimum. These sets were then averaged and fit to a least-squared curve. We found that both minima are shallower in the energy range 53.3–58.3 eV, than those in the range 36.3–44.3 eV. We have determined two critical points, the first at $68.5° \pm 0.3°$, 41.30 ± 0.02 eV, and the second at $143.5° \pm 0.3°$, 37.30 ± 0.02 eV.

The errors shown in tables 4 and 5 are calculated from the relative errors at each point. Relative error was calculated as a square root of the sum of the particular squared relative errors due to: (i) statistical error, (ii) effective path-length correction, (iii) uncertainty of angular scale, and (iv) uncertainty of energy scale. The statistical error was determined for each point in the averaged set according to Poisson statistics. The error due to effective path-length correction is zero for angles at 90°, and it is estimated to be within 1% for the angular range 64°–74° and within 2% for the angular range 135°–150°. Besides statistical error, the error due to the uncertainty in the angular scale has the largest contribution. The precision of the mechanical system gives an uncertainty of 0.1°. The procedure of determining the true zero position from the left–right symmetry in the DCS introduces additional uncertainty of less then 0.2°. So, the overall angular uncertainty was less then 0.3°, which is reflected in the uncertainty in the DCS value ranging from 15% at the

Figure 2. Differential cross sections for elastic electron scattering by argon in the angular range $20°–150°$ at incident energies from 10 to 100 eV: (*a*) three-dimensional representation of the $DCS(E_0, \theta)$ surface shown on a logarithmic scale; (*b*) projection of the $DCS(E_0, \theta)$ surface on the horizontal plane. Numbers correspond to the logarithm of the DCS values in units of 10^{-20} m^2 sr^{-1}.

steepest part of the DCS curve to about 1% at the local extrema points. The uncertainty of the energy scale is determined to be 22 meV. It consists of 7 meV from the instrumental
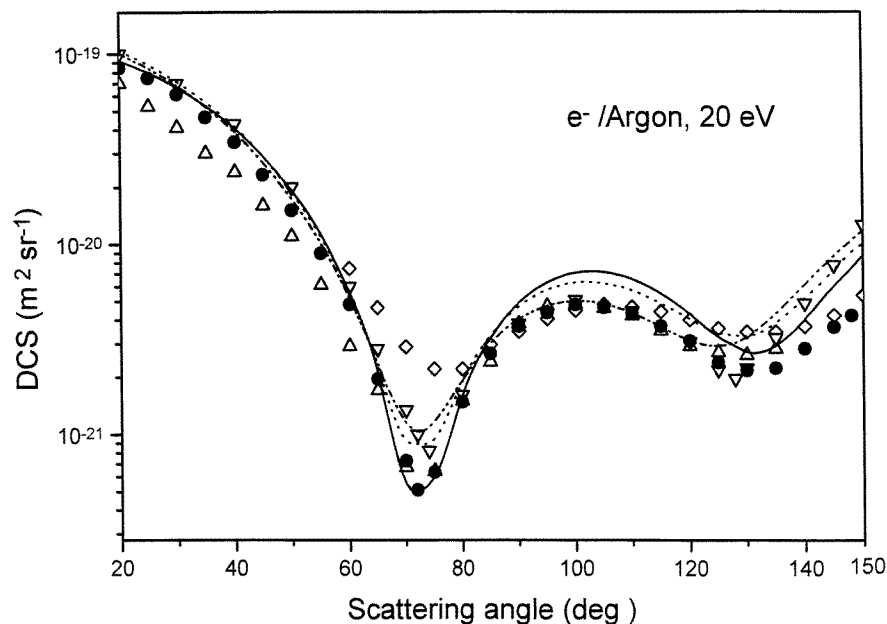
Figure 3. Differential cross sections for elastic electron scattering by argon at 20 eV: ●, our results at 20.3 eV; △, Srivastava *et al* (1981); ▽, Williams and Willis (1975); ◇, Mehr (1967); ——, McEachran and Stauffer (1983); — · —Bartschat *et al* (1988); – – –, Nahar and Wadehra (1987).

Table 5. Elastic differential cross sections for electron scattering by argon in units of 10^{-23} m^2 sr^{-1}. The numbers in parentheses are absolute errors.

θ (deg)	36.3 eV	37.3 eV	38.3 eV	39.3 eV
135	43.9(4.1)	33.6(3.1)	39.4(3.2)	51.9(4.4)
138	24.1(2.9)	18.5(2.3)	22.2(2.2)	31.2(3.3)
140	16.4(2.4)	11.7(1.8)	14.9(1.6)	21.7(2.5)
141	13.8(2.1)	9.4(1.6)	12.5(1.4)	18.3(2.2)
142	11.9(1.9)	7.8(1.4)	10.8(1.2)	15.8(2.0)
142.5	11.3(1.8)	7.3(1.3)	10.3(1.1)	14.8(1.5)
143	10.8(1.8)	7.0(1.2)	10.0(1.1)	14.1(1.9)
143.5	10.4(1.7)	6.8(1.2)	9.8(1.2)	13.6(1.4)
144	10.2(1.7)	6.9(1.2)	9.8(1.3)	13.7(2.0)
144.5	10.2(1.6)	7.1(1.1)	10.0(1.2)	13.2(1.3)
145	10.3(1.5)	7.4(1.1)	10.4(1.2)	13.4(1.7)
148	13.9(1.8)	13.0(1.9)	15.9(1.7)	18.8(2.1)
150	19.1(2.2)	19.2(2.4)	22.4(2.2)	26.8(2.7)
152	26.7(2.8)	27.0(2.7)	30.6(2.7)	38.3(3.2)

calibrations, 5 meV from the fitting of the resonance position in elastic scattering at 28.98 eV, the energy position of which was determined by Dassen *et al* (1983) with an accuracy of 10 meV. This uncertainty is reflected in a relative error of DCS values less than 1%.

The absolute values of the DCSs at each energy are obtained by normalizing our relative DCS values at the local maximum to the interpolated values of available measurements. The
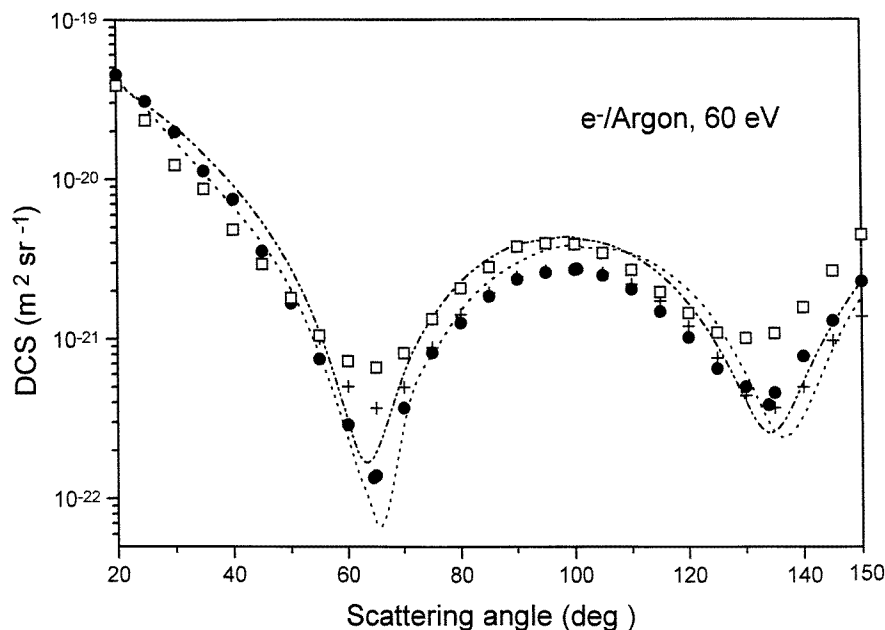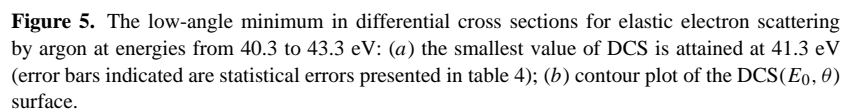
Figure 4. Differential cross sections for elastic electron scattering by argon at 60 eV: ●, our results at 60.3 eV; +, Schackert (1968); □, Vušković and Kurepa (1976); ······, Fon *et al* (1983); —· ·—, Bartschat *et al* (1988).

interpolated curve is smooth which is also confirmed by the Cvejanović and Crowe (1994) measurements from 20 to 110 eV at 90°.

Because 12 incident energies between 10 and 100 eV were included in the first part of this work, we believe that the general energy dependence of the positions of local minima was sufficiently covered in this energy region. Thus, we were able to proceed with the search for the exact minima positions. For the purpose of completeness, in the following discussion we include a few data from the literature at energies below 10 eV.

Angular positions of one low-angle and one high-angle minimum as a function of incident electron energy are shown in figures 7 and 8, respectively. The errors indicated in this experiment are determined as a combination of angular resolution and statistical uncertainty. The positions of minima obtained by other authors are extracted from their DCS results. For the sake of clarity, the comparison was made with selected calculations. Although the integral elastic cross sections according to de Heer *et al* (1979) in the energy range 20–100 eV agree within 10%, DCS data from measurements quoted above may be substantially different. Only experimental results performed with good angular resolution (William and Willis 1975, Srivastava *et al* 1981) (see table 1, group 1) were used for comparison. Other experimental results from table 1 with the limited angular range of measurements or with only a few utilized energies are not presented in the figures.

As one can see from figure 7, the angular position of the low-angle minimum monotonically increases from 57° to 72° as the electron energy decreases from 100 to 20 eV. Calculations by Bartschat *et al* (1994) follow the experimental data, while results of Nahar and Wadehra (1987) (not shown in the figure) and Fon *et al* (1983) increase in steps with a plateau-like shape in this energy range. The position of the minimum at energies below 20 eV was determined with special attention. Numerous repetitions of measurements
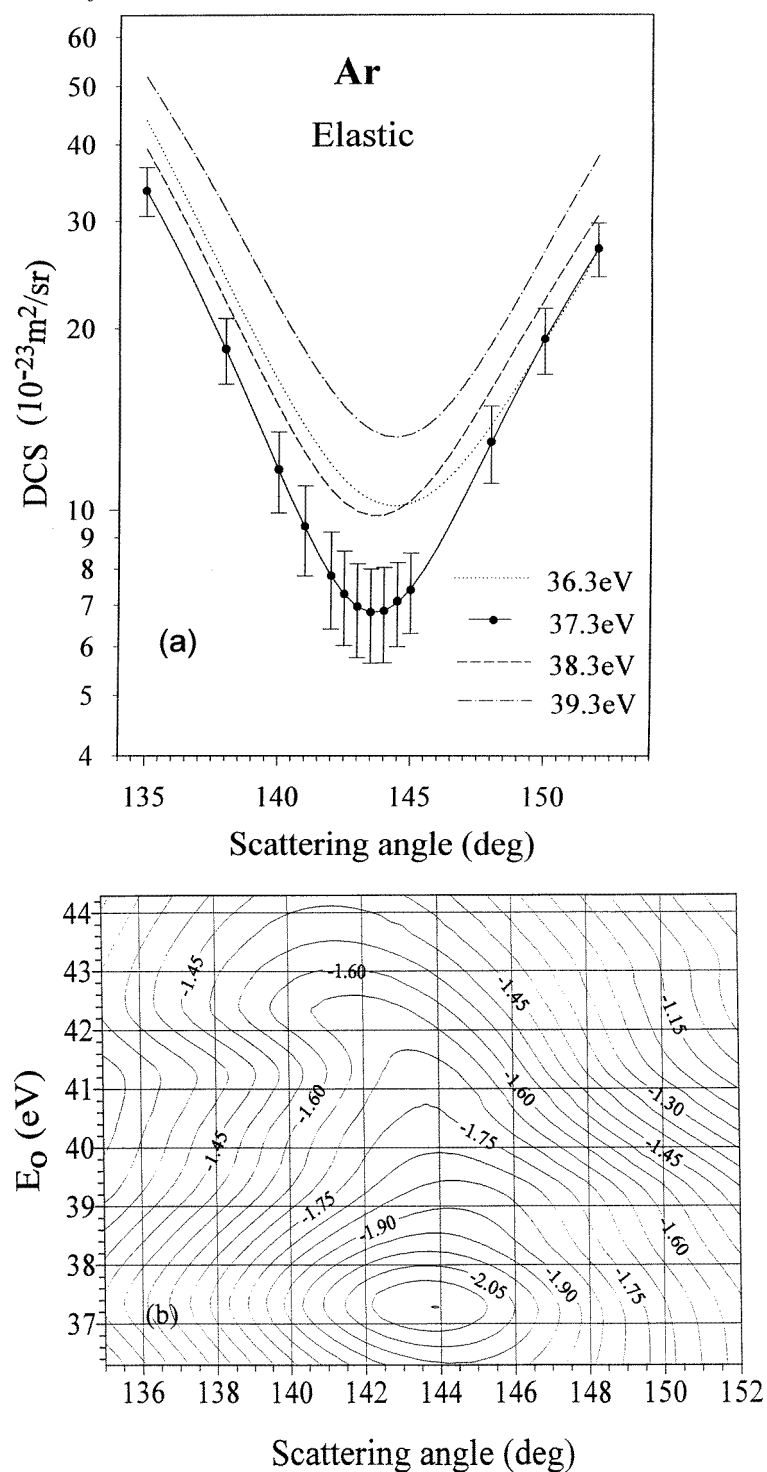
Figure 5. The low-angle minimum in differential cross sections for elastic electron scattering by argon at energies from 40.3 to 43.3 eV: (*a*) the smallest value of DCS is attained at 41.3 eV (error bars indicated are statistical errors presented in table 4); (*b*) contour plot of the DCS(E_0, θ) surface.
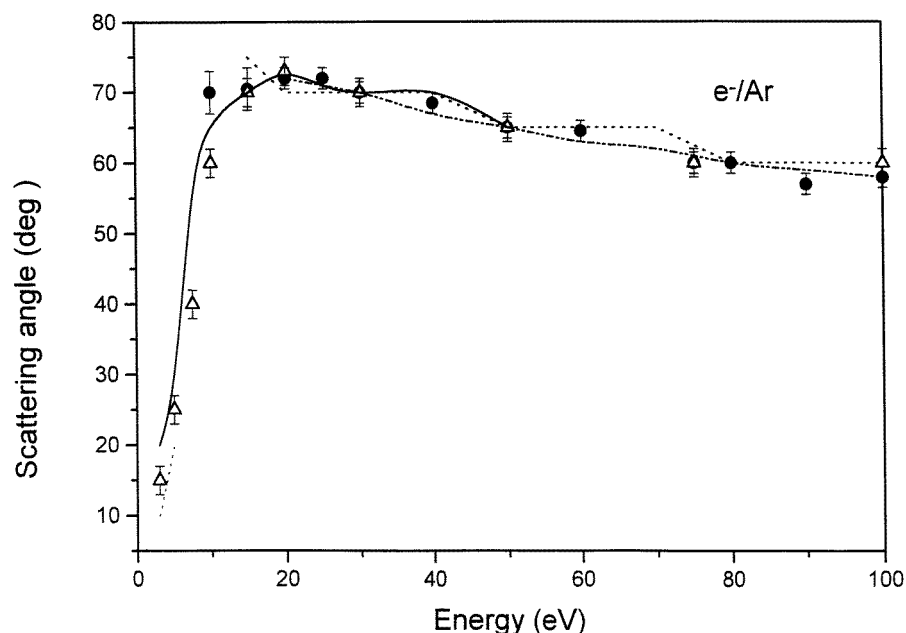
Figure 6. The high-angle minimum in the differential cross section for elastic electron scattering by argon at energies from 36.3 to 39.3 eV: (*a*) the smallest value of DCS is attained at 37.3 eV (error bars indicated are statistical errors presented in table 5); (*b*) contour plot of the DCS(E_0, θ) surface.

Figure 7. Position of low-angle differential cross section minimum versus electron energy in elastic electron scattering by argon: ●, our results; △, Srivastava *et al* (1981) (results from table 2 of that reference); ——, McEachran and Stauffer (1983); ······, Fon *et al* (1983); — · —, Bartschat *et al* (1988). The positions of minima obtained by other authors are extracted from their DCS results.

in this work reconfirm its existence close to 70° at energies just below 20 eV. This fact is of interest for polarization analysis of the scattered electrons. For energies lower than 15 eV the position of the minimum rapidly decreases, reaching a value of 15° for 5 eV electrons. Only the calculations by McEachran and Stauffer (1983) closely follow the experimentally obtained changes in the position of the minimum. In other calculations by Fon *et al* (1983) (shown in the figure) and by Mimnagh *et al* (1993), Nahar and Wadehra (1987), Haberland *et al* (1986) (not shown in the figure) the low-angle DCS minimum disappears at 10 eV.

One can see in figure 8 that the position of the high-angle minimum reaches its largest scattering angle of 143.5° at energies around 40 eV. As mentioned before, this angle is a critical angle at 37.30 eV. As electron energy increases above 40 eV, the position of the minimum decreases almost monotonically to a value of 123° at 100 eV. On the other side, the decrease of electron energy below 37 eV is followed by a rapid lowering of the angle corresponding to the DCS minimum, reaching its lowest value of 115° at 10 eV. In the energy region 37–100 eV, the results of the Bartschat *et al* (1988) calculation follows the experimental data, while results by Nahar and Wadehra (1987), and Fon *et al* (1983) (not shown in the figure) decrease in steps with a plateau-like shape. In the energy region below 37 eV, the calculation by Nahar and Wadehra (1987) follows the experimental results, while the calculation by McEachran and Stauffer (1983) is less sensitive around 10 eV. Agreement with experimental results of Srivastava *et al* (1981) is excellent, except at 30 eV, where the position of the minimum is at an angle higher than 135°, the highest reliable angle in that experiment. Note that the plotted data are taken from table 2 of Srivastava *et al* (1981). The minimum position at 30 eV is confirmed by calculations (see figure 8) and experiment by Williams and Willis (1975), not shown in the figure.
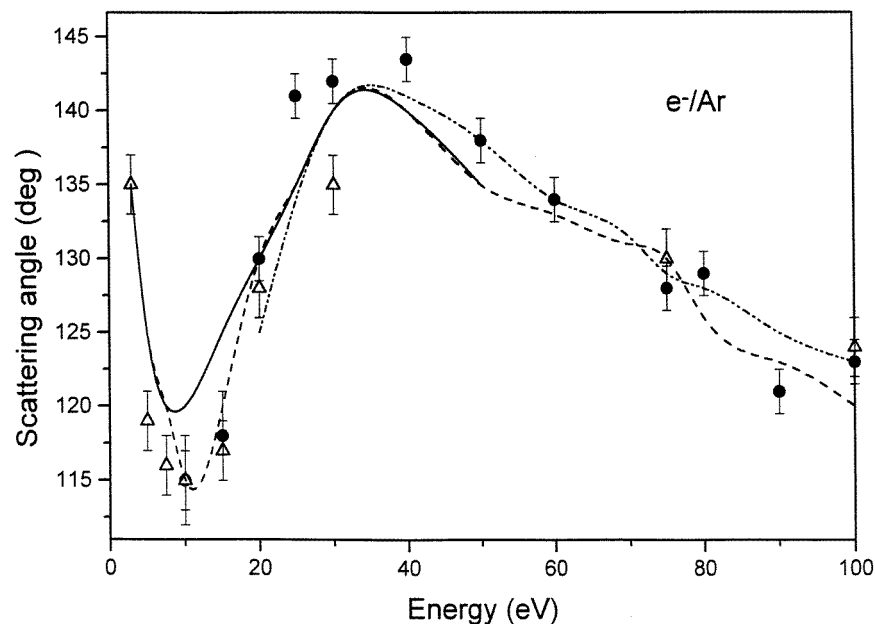
Figure 8. Position of high-angle differential cross section minimum versus electron energy in elastic electron scattering by argon: ●, our results; △, Srivastava *et al* (1981) (results from table 2 of that reference); ——, McEachran and Stauffer (1983); – – –, Nahar and Wadehra (1987); and — · —, Bartschat *et al* (1988). The positions of minima obtained by other authors are extracted from their DCS results.

We would like to point out that Lucas (1979) searched for critical points in electron–argon elastic scattering by compiling available results, while Kessler *et al* (1976) experimentally obtained preliminary results of critical points. To the best of our knowledge, the results of Kessler *et al*, reported at a conference, have not been published in their final form. They reported critical points at: first $65.73° \pm 0.05°$, 56.1 ± 0.7 eV, second $120.90° \pm 0.05°$, 132.3 ± 0.3 eV, and third $143.8° \pm 0.20°$, 42.4 ± 0.9 eV. Only the first and the third point are in the energy domain of this work. The first point corresponds to our critical point at the low-angle minimum. We found unsatisfactory agreement in both the position and energy at which the critical point appears. Because Kessler *et al* found this critical point at 56.1 ± 0.7 eV, we were specially careful in performing the detailed measurements in the energy range 53.3–58.3 eV. As mentioned above, we found that both the low- and high-angle minima are shallower than those around 40 eV, the energy region where our low-angle minimum is located. The third point corresponds to our critical point at the high-angle minimum. We found excellent agreement in the angular position, but our energy was 5 eV lower than that reported in Kessler *et al* (1976).

4. Conclusion

Angular distributions of elastically scattered electrons on argon were measured with good angular resolution in the range 20°–150° where two local minima exist in the energy range 10–100 eV. In this energy range DCS results were obtained for 12 incident electron energies. For the first time results were obtained with good energy and angular resolution at 25, 60, 80, and 90 eV. The results enabled the construction of the more complete three-dimensional

DCS(E_0, θ) surface presented in figure 2, which clearly shows tendencies of DCS changes as a function of incident electron energy and scattering angle. Normalized absolute DCSs are presented in table 2, and at selected energies compared with existing data in figures 3 and 4. At small scattering angles, our data agree with the measurements of Williams and Willis (1975). Also, our results are consistent with the calculation of McEachran and Stauffer (1983). The low- and high-angle minima are as deep as this theory predicts. At 60 eV our result shows deeper minima than the available measurements due to our better angular resolution. Agreement in minima positions with results calculated by Bartschat *et al* (1994) is very good.

Because we made measurements using a large number of incident electron energies and determined both the low- and the high-angle minima positions precisely, we were able to determine accurately the depth and systematic changes in the minima positions with electron energy, as shown in figure 7 and 8. The existence of the first local DCS minimum in the energy region around 10 eV is confirmed by experiments, while it is not predicted by any calculation (Mimnagh *et al* 1993, Nahar and Wadehra 1987, Fon *et al* 1983, Haberland *et al* 1986) except by McEachran and Stauffer (1983). The increase of the angle of the minimum position at 15 eV (Fon *et al* 1983) and at 20 eV (Kemper *et al* 1985) has not been found in any other experiment.

The positions of the DCS minima are of interest for reliable determination of a critical point, i.e. where DCS(E_0, θ) attains its smallest value. We have found two critical points in elastic electron scattering on argon in the energy range 10–100 eV and they are determined to be at $68.5° \pm 0.3°$, 41.30 ± 0.02 eV and at $143.5° \pm 0.3°$, 37.30 ± 0.02 eV. These measurements of minima positions will be an important reference for future calculations. Theoretical attention should be focused on regions where the energy dependence of the angular position of the minima is greatest. In these cases one could expect an increased sensitivity of the calculations to the choice of the interaction potentials.

Acknowledgments

References

Bartschat K, McEachran R P and Stauffer A D 1988 *J. Phys. B: At. Mol. Opt. Phys.* **21** 2789–800
Bartschat K 1994 Private communication
Brinkmann R T and Trajmar S 1981 *J. Phys. E: Sci. Instrum.* **14** 245–55
Bromberg J P 1974 *J. Chem. Phys.* **61** 963–9
Brunt J N H, King J C and Read F H 1977 *J. Phys. B: At. Mol. Phys.* **10** 1289–301
Buckman S J and Clark C W 1994 *Rev. Mod. Phys.* **66** 539–655
Bühring W 1968a *Z. Phys.* **208** 286–98
——1968b *Proc. 4th Int. Conf. Atomic Physics (Heidelberg)* ed J Kowalski and H G Weber (Amsterdam: North-Holland) p 417
Bullard E C and Massey H S W 1931 *Proc. R. Soc.* A **130** 579–90
Crowe A and Cvejanović D 1996 *Can. J. Phys.* **74** 461–7
Cvejanović D and Crowe A 1994 *J. Phys. B: At. Mol. Opt. Phys.* **27** L723–7
——1997 *J. Phys. B: At. Mol. Opt. Phys.* **30** 2873–88
Dassen H W, Gomez R, King J C and McConkey J W 1983 *J. Phys. B: At. Mol. Phys.* **16** 1481–501
de Heer F J, Jansen R H J and van der Kaay W 1979 *J. Phys. B: At. Mol. Phys.* **12** 979–87
Dehmel R C, Fineman M A and Miller D R 1976 *Phys. Rev.* A **13** 115–22

DuBois R D and Rudd M E 1976 *J. Phys. B: At. Mol. Phys.* **9** 2657–67

Filipović D, Marinković B, Pejčev V and Vušković L 1988b *Phys. Rev.* A **37** 356–64

Filipović D, Pejčev V, Marinković B and Vušković L 1988a *Fizika* **20** 421–34

Fon W C, Barrington K A, Burke P G and Hibbert A 1983 *J. Phys. B: At. Mol. Phys.* **16** 307–21

Furst J E, Golden D E, Mahgerefteh M, Zhou J and Mueller D 1989 *Phys. Rev.* A **40** 5592–600

Gibson J C, Gulley R J, Sullivan J P, Buckman S J, Chan V and Burrow P D 1996 *J. Phys. B: At. Mol. Opt. Phys.* **29** 3177–95

Gupta S C and Rees J A 1975 *J. Phys. B: At. Mol. Phys.* **8** 1267–74

Haberland R, Fritsche L and Noffke J 1986 *Phys. Rev.* A **33** 2305–14

Haddad G N and O'Malley T F 1982 *Aust. J. Phys.* **35** 35–9

Hughes A L and McMillen J H 1932 *Phys. Rev.* **39** 585–600

Ihra W and Friedrich H 1992 *Phys. Rev.* A **45** 5278–81

Jansen R H J, de Heer F J, Luyken H J, van Wingerden B and Blaauw H J 1976 *J. Phys. B: At. Mol. Phys.* **9** 185–212

Kemper F, Rosicky F and Feder R 1985 *J. Phys. B: At. Mol. Phys.* **18** 1223–8

Kessler J, Liedtke J and Lukas C B 1976 *Physics of Ionized Gases (Dubrovnik)* ed B Navinšek (Ljubljana: J Stefan Institute) p 61

Khare S P and Raj D 1980 *J. Phys. B: At. Mol. Phys.* **13** 4627–32

Lewis B R, Furness J B, Teubner P J O and Weigold E 1974 *J. Phys. B: At. Mol. Phys.* **7** 1083–90

Lucas C B 1979 *J. Phys. B: At. Mol. Phys.* **12** 1549–58

Marinković B, Pejčev V, Filipović D and Vušković L 1983 *Proc. 13th Int. Conf. Physics of Electronic and Atomic Collisions (Berlin)* ed J Eichler, W Fritsch, I V Hertel, N Stolterhoft and U Wille (Amsterdam: North-Holland) p 85

McEachran R P and Stauffer A D 1983 *J. Phys. B: At. Mol. Phys.* **16** 4023–38

Mehr J 1967 *Z. Phys.* **198** 345–50

Mimnagh D J R, McEachran R P and Stauffer A D 1993 *J. Phys. B: At. Mol. Opt. Phys.* **26** 1727–41

Nahar S N and Wadehra J M 1987 *Phys. Rev.* A **35** 2051–64

Panajotović R, Minić M, Marinković B, Pejčev V and Filipović D 1994 *Proc. 17th Symp. Physics of Ionized Gases (Belgrade)* ed by B Marinković and Z Lj Petrović (Belgrade: Institue of Physics) p 16

Plenkiewicz B, Plenkiewicz P and Jay-Gerin J-P 1988 *Phys. Rev.* A **38** 4460–9

Qing Z, Beerlage M G M and van der Wiel M J 1982 *Physica* C **113** 225–36

Read F H, Brunt J N H and King J C 1976 *J. Phys. B: At. Mol. Phys.* **9** 2209–19

Register D F, Vušković L and Trajmar S 1986 *J. Phys. B: At. Mol. Phys.* **19** 1685–97

Roy D and Carette J D 1975 *J. Phys. B: At. Mol. Phys.* **8** L157–60

Saha H P 1991 *Phys. Rev.* A **43** 4712–22

Sanche L and Schulz G J 1972 *Phys. Rev.* A **5** 1672–83

Schackert K 1968 *Z. Phys.* **213** 316–22

Sienkiewicz J E and Baylis W E 1987 *J. Phys. B: At. Mol. Phys.* **20** 5145–56

Srivastava S K, Tanaka H, Chutjian A and Trajmar S 1981 *Phys. Rev.* A **23** 2156–66

Vušković L and Kurepa M V 1976 *J. Phys. B: At. Mol. Phys.* **9** 837–42

Walker D W 1971 *Adv. Phys.* **20** 257–323

Weyhreter M, Barzick B, Mann A and Linder F 1988 *Z. Phys.* D **7** 333–43

Williams J F and Willis B A 1975 *J. Phys. B: At. Mol. Phys.* **8** 1670–82